

## FINE PARTICLE EMISSIONS FROM RESIDUAL FUEL OIL COMBUSTION: CHARACTERIZATION AND MECHANISMS OF FORMATION

WILLIAM P. LINAK,<sup>1</sup> C. ANDREW MILLER<sup>1</sup> AND JOST O. L. WENDT<sup>2</sup>

<sup>1</sup>*Air Pollution Prevention and Control Division, MD-65*

*National Risk Management Research Laboratory*

*U.S. Environmental Protection Agency*

*Research Triangle Park, NC 27711, USA*

<sup>2</sup>*Department of Chemical and Environmental Engineering*

*University of Arizona*

*Tucson, AZ 85721 USA*

The characteristics of particulate matter (PM) emitted from residual fuel oil combustion in two types of combustion equipment were compared. A small commercial 732 kW rated fire-tube boiler yielded a weakly bimodal particulate size distribution (PSD) with over 99% of the mass contained in a broad coarse mode and only a small fraction of the mass in an accumulation mode consistent with ash vaporization. Bulk samples collected and classified by a cyclone indicate that 30% to 40% of the total particulate emissions were less than 2.5  $\mu\text{m}$  aerodynamic diameter ( $\text{PM}_{2.5}$ ). The coarse mode PM was rich in char, indicating relatively poor carbon burnout, although calculated combustion efficiencies exceeded 99%. This characteristic behavior is typical of small fire-tube boilers.

Larger, utility-scale units firing residual oil were simulated using an 82 kW rated laboratory-scale refractory-lined combustor. Particulate matter emissions from this unit were in good agreement with published data including published emission factors. These data indicated that the refractory-lined combustor produced less total but more fine particulate emissions, as evident from a single unimodal PSD centered at  $\sim 0.1 \mu\text{m}$  diameter. Bulk cyclone segregated samples indicated that here all the PM were smaller than 2.5  $\mu\text{m}$  aerodynamic diameter, and loss on ignition (LOI) measurements suggested almost complete char burnout. These findings are interpreted in the light of possible mechanisms governing the release of organically bound refractory metals and may have particular significance in considering the effects of fuel oil combustion equipment type on the characteristic attributes of the fine PM emitted into the atmosphere and their ensuing health effects.

### Introduction

Airborne fine particulate matter (PM) has recently become the subject of considerable environmental interest due to the results of a number of studies correlating short-term exposures to ambient levels of fine PM with acute adverse health effects [1–4]. Consequently, ambient concentrations and source emissions of PM less than 2.5  $\mu\text{m}$  in diameter ( $\text{PM}_{2.5}$ ) face the possibility of increased regulation [5]. Numerous causative theories exist; however, health effect researchers have identified at least two properties of ambient particle composition that appear to exacerbate health damage. These are the presence of transition metals (e.g., Cu, Fe, V, Ni, and Zn) [6,7] and aerosol acidity. In addition to particle composition, another apparent factor influencing health impact is the presence of ultrafine particles ( $< 0.1 \mu\text{m}$  in diameter) [2]. All three characteristics, transition metals, acidity, and ultrafine size, are exhibited by the PM generated from the combustion of residual fuel oils. Hence, one might hypothesize

residual fuel oil combustion to be suspect, as far as emission of toxic fine particles is concerned. Building upon previous work examining the effects of fuel oil compositions on the physical and chemical characteristics of fine PM [8], this paper describes the effects of different combustion equipment types. The results of both studies can be used as the basis for ultimately linking measures of acute pulmonary damage to combustion engineering variables.

### Experimental

Particle characteristics and emissions were compared from two types of combustion systems. These can be considered to represent the extremes of a range of practical conditions under which fuel oil is burned. Although they may not represent specific boilers in all respects, they were investigated here with a view to determining how this range of combustion conditions influences fine PM characteristics and formation mechanisms. The first system was a

# Report Documentation Page

*Form Approved*  
*OMB No. 0704-0188*

Public reporting burden for the collection of information is estimated to average 1 hour per response, including the time for reviewing instructions, searching existing data sources, gathering and maintaining the data needed, and completing and reviewing the collection of information. Send comments regarding this burden estimate or any other aspect of this collection of information, including suggestions for reducing this burden, to Washington Headquarters Services, Directorate for Information Operations and Reports, 1215 Jefferson Davis Highway, Suite 1204, Arlington VA 22202-4302. Respondents should be aware that notwithstanding any other provision of law, no person shall be subject to a penalty for failing to comply with a collection of information if it does not display a currently valid OMB control number.

1. REPORT DATE <b>04 AUG 2000</b>	2. REPORT TYPE <b>N/A</b>	3. DATES COVERED <b>-</b>			
4. TITLE AND SUBTITLE <b>Fine Particle Emissions from Residual Fuel Oil Combustion: Characterization and Mechanisms of Formation</b>		5a. CONTRACT NUMBER			
		5b. GRANT NUMBER			
		5c. PROGRAM ELEMENT NUMBER			
6. AUTHOR(S)		5d. PROJECT NUMBER			
		5e. TASK NUMBER			
		5f. WORK UNIT NUMBER			
7. PERFORMING ORGANIZATION NAME(S) AND ADDRESS(ES) <b>Air Pollution Prevention and Control Division, MD-65 National Risk Management Research Laboratory U.S. Environmental Protection Agency Research Triangle Park, NC 27711, USA</b>		8. PERFORMING ORGANIZATION REPORT NUMBER			
		10. SPONSOR/MONITOR'S ACRONYM(S)			
9. SPONSORING/MONITORING AGENCY NAME(S) AND ADDRESS(ES)		11. SPONSOR/MONITOR'S REPORT NUMBER(S)			
		12. DISTRIBUTION/AVAILABILITY STATEMENT <b>Approved for public release, distribution unlimited</b>			
13. SUPPLEMENTARY NOTES <b>See also ADM001790, Proceedings of the Combustion Institute, Volume 28. Held in Edinburgh, Scotland on 30 July-4 August 2000.</b>					
14. ABSTRACT					
15. SUBJECT TERMS					
16. SECURITY CLASSIFICATION OF:			17. LIMITATION OF ABSTRACT <b>UU</b>	18. NUMBER OF PAGES <b>8</b>	19a. NAME OF RESPONSIBLE PERSON
a. REPORT <b>unclassified</b>	b. ABSTRACT <b>unclassified</b>	c. THIS PAGE <b>unclassified</b>			

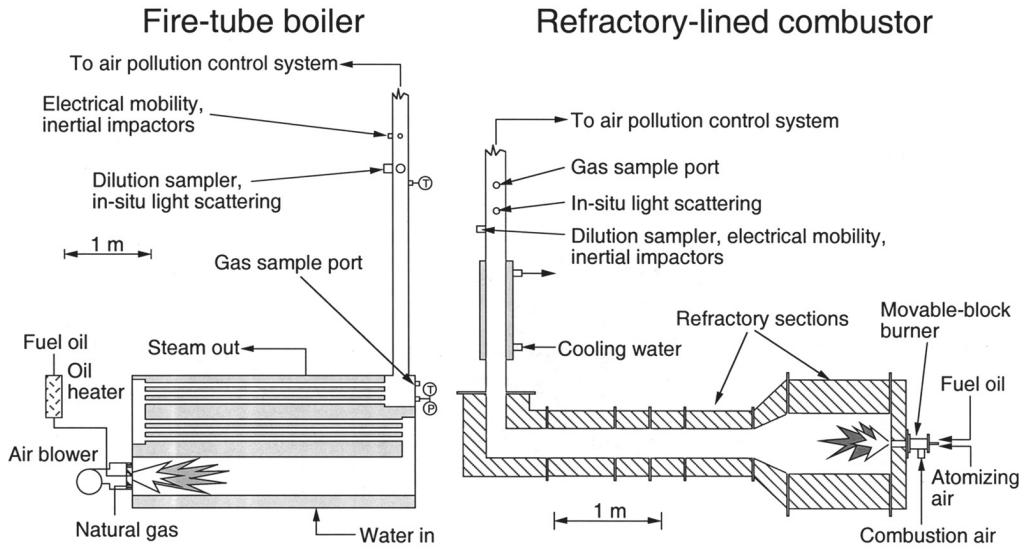


FIG. 1. Two EPA combustion systems.

small fire-tube boiler, in which combustion occurs in tubes surrounded by water or steam. Such small boilers have large heat transfer surfaces, small volumes, relatively short residence times ( $\sim 2$  s), cold walls, high gas-quenching rates ( $\sim 500$  K/s), and often produce emissions with relatively high carbon contents due to unburned carbonaceous char. The second system was a laboratory-scale, refractory-lined combustor designed to simulate the time/temperature environments of larger utility boilers and incinerators. In large utility boilers, the water or steam, rather than the combustion gases, is contained in tubes. These systems, including the refractory-lined combustor, operate at higher temperatures with lower quenching rates ( $\sim 200$  K/s) and longer residence times ( $\sim 6$  s). As is discussed later, particle emissions from this system contain very little unburned carbon and better approximate emissions from large oil-fired utility boilers, as reported in the literature. Based on extrapolation of temperature measurements made at axial locations downstream, peak temperatures for the refractory-lined combustor were between 1700 and 1900 K. Peak temperatures for the fire-tube boiler were  $\sim 500$  K lower.

#### Fire-Tube Boiler

Experiments were performed using the commercially available, North American, three-pass, fire-tube package boiler shown in Fig. 1. This unit was equipped with a 732 kW rated (586 kW operated) North American burner with an air-atomizing oil nozzle. Oil temperature and oil and atomizing air pressures were independently controlled to ensure proper oil atomization. Fig. 1 indicates the locations

of several sampling ports. Temperatures at these locations ranged from 450 to 550 K. Additional system details have been presented elsewhere [8].

#### Refractory-Lined Combustor

Figure 1 also shows the laboratory-scale, refractory-lined combustor. This research unit is designed to simulate the time/temperature and mixing characteristics of practical gas- and oil-fired combustion systems. The refractory-lined combustor was equipped with a 82 kW rated (59 kW operated) International Flame Research Foundation (IFRF) moveable-block, variable-air swirl burner which incorporated an air-atomizing oil nozzle positioned along its center axis and annular swirling air to promote flame stability (IFRF type 2 flame, swirl = 1.48). Gas and aerosol samples were taken from stack locations at temperatures of  $\sim 670$  K.

#### Particulate Sampling and Analysis

Standard U.S. Environmental Protection Agency (EPA) methods 5 and 60 sampling and analytical procedures were used to determine total particulate and metal concentrations [9–11] using inductively coupled argon plasma atomic emissions spectrometry (ICP-AES). Other metal analyses were determined by X-ray fluorescence (XRF) spectroscopy. Additional samples were analyzed by X-ray absorption fine structure (XAFS) spectroscopy, an element-specific structural analysis that is useful for determining trace element speciation and forms of occurrence in complex materials such as combustion ash [12,13].

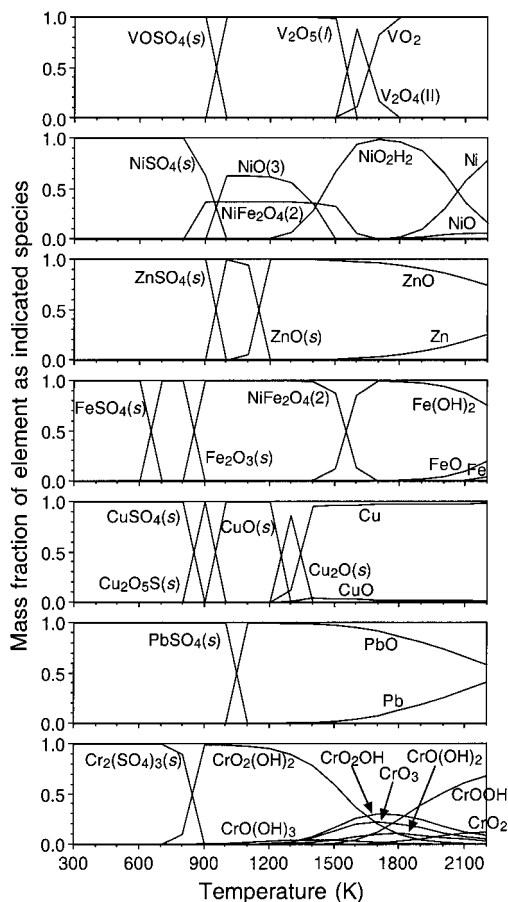


FIG. 2. Residual fuel oil equilibrium predictions.

Particle size distributions (PSDs) were determined by three techniques: electrical mobility and inertial impaction for sampled aerosols, and light scattering for *in situ* in-stack analyses. Extractive samples were taken for inertial impaction and electrical mobility analyses using an isokinetic aerosol sampling system described elsewhere [14]. These diluted samples were directed to a TSI Inc. scanning mobility particle sizer (SMPS) configured to yield 54 channels, evenly spaced (logarithmically) over a 0.01 to 1.0  $\mu\text{m}$  diameter range. Samples extracted during the fire-tube boiler experiments were directed to an Andersen Inc. eight-stage, 25 L/min, atmospheric pressure, in-stack cascade impactor. An MSP Inc. 10-stage, 30 L/min micro-orifice uniform deposit impactor (MOUDI) was used during the refractory-lined combustor experiments. *In situ* light-scattering PSDs were obtained using an Insitex Inc. particle counter sizer velocimeter with a working range of  $\sim 0.3$  to 100  $\mu\text{m}$  diameter, which slightly overlapped and extended the PSD data collected by the SMPS.

Large quantities of size-segregated PM were collected for parallel toxicological studies and XAFS analyses using a non-isokinetic 0.28  $\text{m}^3/\text{min}$  dilution sampler [15]. The extracted sample passed through a cyclone (50% and 90% collection efficiencies for 1.8 and 2.5  $\mu\text{m}$  diameter PM, respectively) and was then diluted with clean filtered ambient air (2.8  $\text{m}^3/\text{min}$ ) to approximately ambient temperature ( $\sim 3$  s residence time). The resulting PM was collected on 64.8 cm diameter Teflon-coated glass fiber filters, transferred to sampling jars, and made available for subsequent chemical, physical, and toxicological analysis.

The No. 6 oil used in both experimental systems contained 2.33% sulfur and 0.1% ash. Operational characteristics for both systems included similar oil temperatures (380–400 K), atomizing air pressures (200–240 kPa), and stoichiometries ( $\text{SR} = 1.2$ ). The droplet PSD produced by the fire-tube boiler's Delavan Airo Combustion air-atomizing oil nozzle (model 30615-84) was measured using a PSA-32 particle size analyzer and produced a relatively narrow PSD with a mean diameter between 30 and 40  $\mu\text{m}$ . The refractory-lined combustor experiments used a similar Spraying Systems Co. (model Air Atom 1/4-JSS) air-atomizing oil nozzle designed to produce similar droplet PSDs. Therefore, any differences in carbon burnout may be attributed to differences in temperature history rather than droplet size.

## Results and Discussion

### Equilibrium Predictions

Although numerous previous studies reported on equilibrium predictions in combustion environments, there are relatively few results for the inorganic ash species and concentrations pertinent to residual oil combustion. Thermochemical predictions were determined using the Chemical Equilibrium Analysis (CEA) computer code for calculating complex chemical equilibrium compositions [16], with thermochemical data taken from the literature [17–24]. Of interest is the predicted partitioning between vapor and condensed phases, as well as elemental speciation. The fuel ultimate analysis and trace element concentrations were taken from Miller et al. [8]. However, only trace elements with concentrations greater than 1  $\mu\text{g/g}$  of oil were considered in the calculations.

Figure 2 presents the results for seven trace elements. Mass fractions of the elements (as indicated species) are plotted against temperature. The calculated elemental dew points range from 1800 K for V to 900 K for Cr. These predictions indicate that all seven elements might vaporize within the refractory-lined combustor, although the predicted dew points for V, Ni, and Fe are similar to the estimated

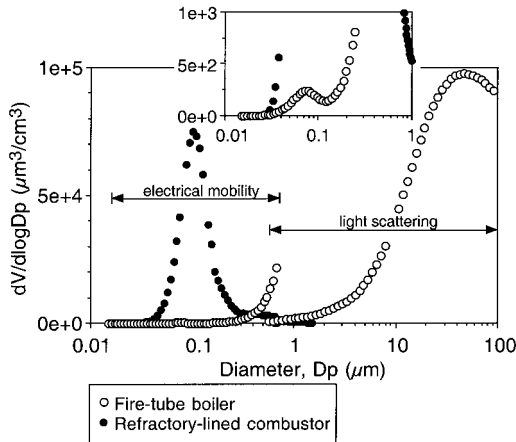


FIG. 3. Measured volume PSDs.

peak temperature. These dew points are lower than those calculated for pulverized coal and incineration applications because of the low ash and metal concentrations [25]. All seven elements are predicted to form sulfates at lower temperatures (700–1100 K), and this may affect the solubility and perhaps the bioavailability and toxicity associated with these trace elements.

#### Particle Size Distributions

Figure 3 presents representative volume PSDs for the fire-tube boiler (open symbols) and refractory-lined combustor (shaded symbols) experiments. With additional detail shown in the inset, these electrical mobility and light-scattering measurements span four orders of magnitude of particle diameter (0.01–100  $\mu\text{m}$ ). The fire-tube boiler PSDs indicate that most of the particle volume is associated with large (coarse mode) particles ( $>10 \mu\text{m}$  diameter). However, the inset shows that even the fire-tube boiler (open symbols) produces a small accumulation mode with a mean diameter between 0.07 and 0.08  $\mu\text{m}$ . This mode is notably smaller than that of the refractory-lined combustor (shaded symbols). Thus, both configurations produced an ultrafine mode, but only the fire-tube boiler produced a bimodal PSD with a large and dominant coarse mode.

This type of bimodal PSD is consistent with a mechanism of metal vaporization/nucleation/coagulation/condensation and incomplete burnout of residual fuel cenospheres [8]. According to Williams [26], as atomized fuel oil droplets ( $<10$  to  $\sim 100 \mu\text{m}$  in diameter) are heated, the lighter organic components vaporize, diffuse into the gas phase, and react (self-ignite), forming diffusion flames around each droplet. As the process proceeds, fractional distillation, liquid-phase cracking, and thermal decomposition add vapor-phase fuel species to the flame

front, causing considerable swelling of the remaining heavy tar droplet. As the volatile components are depleted, the remaining heavy tars collapse to form a carbonaceous residue (or char cenosphere) with an open cell structure. The flame front recedes into the cenosphere, resulting in heterogeneous combustion at a rate of about one-tenth that of the initial droplet. These porous particles, composed primarily of carbon and ash, may be quite large (comparable or even larger than the original fuel droplet). As oxygen diffuses into the cenospheres, heterogeneous combustion results in high internal temperatures that promote vaporization of the inherent (organically bound) mineral matter. If quenching interrupts combustion before char oxidation is complete, the remaining cenospheres contribute to the supermicron PSD.

Scanning electron microscope images of oil char collected from the fire-tube boiler showed a sponge-like morphology that clearly suggests swelling and extensive pore formation. It is apparent that the extent of ash (metal) vaporization depends on the thermal environment and the extent of carbon burnout. For incomplete char combustion, even in cases where combustion efficiencies exceed 99%, a substantial fraction of the trace metals remain trapped within unburned char particles. However, those trace elements which vaporize subsequently nucleate to form new particles as they diffuse away from the locally reducing environment inside the char particles. The distinctive submicron peak (between 0.07 and 0.08  $\mu\text{m}$  in diameter) is clearly indicative of particles formed by nucleation, coagulation, and condensation of vaporized materials. Thus, when large portions of the metal constituents fail to vaporize (open symbols), the accumulation mode will be very much smaller than when they do vaporize (shaded symbols). It is unlikely that the inherently bound ash components vaporize continuously throughout the char combustion process to be recaptured by other char particles before nucleating. This is because the high species dew points and quench rates, the low number concentrations and available surfaces offered by char particles, and the relatively cool highly oxidizing environment between char particles all promote nucleation rather than surface condensation. Once nucleated, nuclei-char interactions cannot explain the measured PSDs.

The refractory-lined combustor volume PSD (shaded symbols) consists exclusively of a narrow submicron accumulation mode with a mean diameter of  $\sim 0.1 \mu\text{m}$ . Both light-scattering measurements and the lack of any cyclone catch containing gray or black particles with measurable loss on ignition (LOI) support this. Clearly, as the char is consumed, the metals have vaporized almost completely and subsequently nucleated and grown to form the distinctive accumulation mode shown in Fig. 3. Comparison between the areas under the submicron volume PSD for the two types of equipment suggests

TABLE 1  
Comparison of calculated mass concentrations determined from measured volume PSDs with measured mass concentrations determined by EPA method 5

	Measured Volume Conc. ( $\mu\text{m}^3/\text{cm}^3$ )	Calculated Mass Conc. ( $\text{mg}/\text{m}^3$ ) <sup>a</sup>	Measured Mass Conc. ( $\text{mg}/\text{m}^3$ ) <sup>b</sup>
<b>Boiler</b>			
SMPS	8.8e + 1	0.31	—
INSITEC	9.8e + 4	180	—
Total	9.8e + 4	180	184 (6.2) <sup>c</sup>
<b>Combustor</b>			
SMPS	2.7e + 4	93	—
INSITEC	1.9e + 2	0.36	—
Total	2.7e + 4	93	93

<sup>a</sup>Assumed fine mode particle density =  $3.5 \text{ g}/\text{cm}^3$  based on typical densities for vanadium species. Assumed coarse mode particle density =  $1.85 \text{ g}/\text{cm}^3$ .

<sup>b</sup>Measured mass concentrations determined using EPA method 5[11].

<sup>c</sup>Number in parentheses indicated standard deviation based on multiple measurements.

that, while only a very small fraction ( $<1\%$ ) of the metal trace elements are vaporized in the fire-tube boiler, well over 99% of these constituents vaporize in the refractory-lined combustor.

#### Comparison of Calculated and Measured Mass Concentrations

Total mass concentrations were calculated by integrating measured volume PSDs and applying assumptions on appropriate densities and were compared to mass concentrations measured independently (Table 1). Particle densities of  $3.5$  and  $1.85 \text{ g}/\text{cm}^3$  were chosen for the accumulation (SMPS) and coarse (INSITEC) modes, respectively, based on average densities of trace element sulfates and oxides and activated carbons and oil chars taken from the literature. The calculated mass concentrations of  $180$  and  $93 \text{ mg}/\text{m}^3$  for the boiler and the combustor, respectively, agree remarkably well with the independently measured mass concentrations of  $184$  and  $93 \text{ mg}/\text{m}^3$  for the boiler and the combustor experiments, respectively.

#### Elemental Composition and Particle Size

As expected, trace element measurements showed similar mass emissions for both the fire-tube boiler and the refractory-lined combustor experiments (data not reported here). However, PM from the

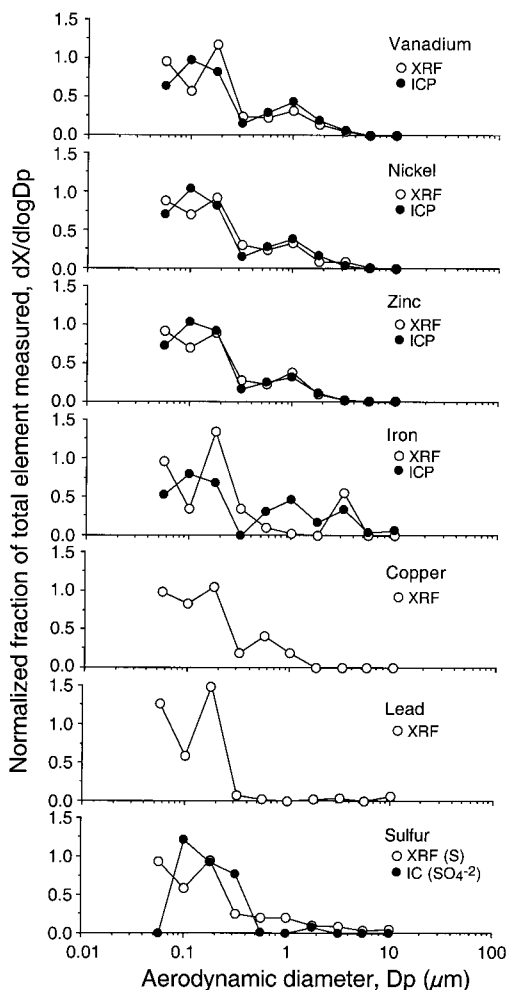


FIG. 4. Elemental PSDs from the refractory-lined combustor.

fire-tube boiler had high LOI values ranging from 60% to 85%, while the refractory-lined combustor samples did not. For the latter, the sum of V, Ni, Zn, Fe, Cu, Pb, and S, as elements, account for  $21.6 \text{ mg}/\text{m}^3$ , or 23%, of the total mass emissions; whereas, when counted as sulfates, they account for  $67.1 \text{ mg}/\text{m}^3$ , or  $\sim 72\%$ , of the total mass emissions. XAFS spectroscopy indicated that, while a large portion (40%–60%) of the sulfur measured in the fire-tube boiler PM existed as unoxidized organic sulfur (predominantly thiophenic sulfur), essentially all (99%) of the particulate-bound sulfur in the refractory-lined combustor samples had been oxidized to form sulfates.

Figure 4 presents elemental mass fractions versus particle diameter for six metals and sulfur from the

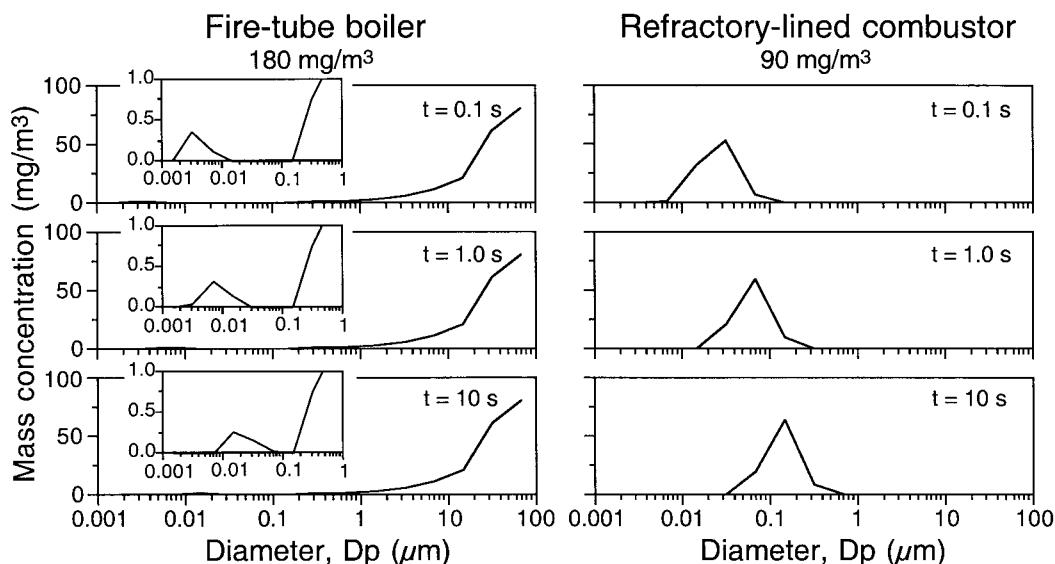


FIG. 5. Predicted evolution of PSDs by coagulation.

refractory-lined combustor tests. Metals were analyzed by XRF and ICP-AES, while sulfur and sulfates were determined by XRF and ion chromatography (IC), respectively. In general, XRF and ICP-AES analyses produced similar results, and the emissions of these elements were concentrated in particles between  $\sim 0.08$  and  $0.2 \mu\text{m}$  in diameter (i.e., the accumulation mode shown in Fig. 3). Sulfur and sulfates were present within particles of the same size.

#### Model Predictions

Experimental results were compared to model predictions using a multicomponent aerosol simulation code (MAEROS) [27]. The purpose of these calculations was to illustrate that the resulting PSDs for both systems could be predicted using the same modeling approach involving char particle burnout (or premature quenching) followed by homogeneous nucleation and coagulation of a portion of the PM mass. A secondary objective was to determine the extent to which differences in coagulation rates caused by large differences in vaporized mass and resulting number densities might account for the differences in the measured PSDs. Details regarding the application of MAEROS to combustion environments can be found elsewhere [28]. Fig. 5 illustrates the predicted PSD evolution for both the fire-tube boiler and refractory-lined combustor. Coagulation was the only mechanism considered.

To examine particle evolution within the fire-tube boiler, 99.8% of the  $180 \text{ mg/m}^3$  PM mass was distributed among 13 sections (within MAEROS) so as

to simulate the coarse mode mass PSD illustrated in Fig. 3. The remaining 0.2% of this mass was assigned to section 2 ( $0.0021\text{--}0.0046 \mu\text{m}$  in diameter) to simulate the nucleation of a vapor fume (see Table 1). The initial number concentration was  $1.5 \times 10^{16}/\text{m}^3$ , with the nucleating vapor accounting for well over 99.99% of these particles. System pressure and temperature were maintained at  $1.01 \times 10^5 \text{ Pa}$  and  $810 \text{ K}$ , respectively, to simulate postflame conditions. Following this initial distribution, Fig. 5 presents calculated mass PSDs at 0.1, 1.0, and 10 s. While these three PSDs also represent  $180 \text{ mg/m}^3$ , number concentrations decline as coagulation proceeds. At 1.0 and 10.0 s, the coagulating nuclei have grown into the  $0.01$  to  $0.1 \mu\text{m}$  diameter range. These times represent a range of typical residence times within combustion systems. At 10 s, number concentrations have fallen to  $1.2 \times 10^{14}/\text{m}^3$ , and the coagulating nuclei are accumulating in a mode with a mean diameter of  $\sim 0.02 \mu\text{m}$  (see Fig. 5). The distribution of the coarse mode PM is relatively unaffected by these processes.

In contrast to the boiler simulation, 100% of the  $90 \text{ mg/m}^3$  PM mass measured in the refractory-lined combustor was assigned to section 2. Again, this initial distribution corresponds to the partitioning seen in Table 1 and indicates complete oxidation of the oil char and vaporization of the inorganic elements followed by homogeneous nucleation. The initial number concentration is  $2.7 \times 10^{15}/\text{m}^3$ . In comparison to the boiler simulation, Fig. 5 indicates that these nuclei tend to coagulate much more quickly, due to larger number concentrations. At 1 and 10 s, as number concentrations fall to  $8.2 \times 10^{14}$  and  $7.6$

$\times 10^{13}/\text{m}^3$ , respectively, coagulation slows considerably causing the aerosol to accumulate into a mode between  $\sim 0.07$  and  $0.2 \mu\text{m}$  in diameter. Coagulation processes predict that the accumulation mode produced from the refractory-lined combustor would have a larger mean diameter compared to the accumulation mode produced from the fire-tube boiler. This prediction is reflected in the measurements. The accumulation mode measured from the refractory-lined combustor matches the predicted PSD, while the predicted accumulation mode for the fire-tube boiler ( $0.02 \mu\text{m}$  in diameter) slightly underpredicts the measured value ( $\sim 0.07 \mu\text{m}$  diameter). Heterogeneous condensation of a portion of the vapor on existing nuclei is a competing process and has been shown to increase particle growth rates [29]. Additionally, the coagulation mechanism does not include the effect of differing fractal properties of any agglomerates that may be formed. It has been assumed here that only spheres result from the coagulation process.

### Conclusions

The effects of combustion configuration on fine particle emissions from residual fuel oil combustion were examined. A laboratory-scale, refractory-lined combustor, which was shown to simulate combustion conditions of a utility-scale, residual oil-fired boiler (as far as particulate emission factors were concerned), produced an essentially unimodal PSD with a mean diameter of  $\sim 0.1 \mu\text{m}$ . Conversely, a commercial fire-tube package boiler produced particles with a weak bimodal PSD, which included a small fraction ( $\sim 0.2\%$ ) of the particle mass with diameters below  $0.1 \mu\text{m}$  and a large fraction ( $\sim 99.8\%$ ) of the particle mass with diameters between  $0.5$  and  $100 \mu\text{m}$ . The ultrafine particles from both combustion systems were consistent with the accumulation of an evolving aerosol formed by the nucleation of vapor-phase metal sulfates. The large particles from the fire-tube boiler were shown to consist of large porous carbonaceous cenospheres resulting from incomplete char burnout, and this characteristic is not uncommon for that class of equipment.

Ash vaporization and ultrafine particle formation is highly dependent on the thermal environment and extent of char burnout, with most trace element vaporization occurring late in the char oxidation process. Although the total particulate mass concentrations from the refractory-lined combustor was less than half that of the fire-tube boiler, ultrafine particle concentrations for the refractory-lined combustor were notably larger than those measured for the fire-tube boiler. Volume PSDs obtained from two independent particle sizing instruments were, with only a few very reasonable assumptions, consistent with independently measured total mass emission rates, for both equipment types.

### Acknowledgments and Disclaimer

Portions of this work were conducted under P.O. SCR244NASX with J. O. L. Wendt and contract 68-C-99-201 with ARCADIS Geraghty & Miller. The research described in this article has been reviewed by the Air Pollution Prevention and Control Division, U.S. EPA, and approved for publication. The contents of this article should not be construed to represent Agency policy nor does mention of trade names or commercial products constitute endorsement or recommendation for use.

### REFERENCES

1. Wilson, R., and Spengler, J. D., eds., *Particles in Our Air: Concentrations and Health Effects*, Harvard University Press, Cambridge, MA, 1996.
2. U.S. EPA, *Air Quality Criteria for Particulate Matter*, EPA-600/P-99/002 (NTIS PB2000-108516), National Center for Environmental Assessment, Research Triangle Park, NC, 1999.
3. Bachmann, J. D., Damberg, R. J., Caldwell, J. C., Edwards, C., and Koman, P. D., *Review of the National Ambient Air Quality Standards for Particulate Matter: Policy Assessment of Scientific and Technical Information*, EPA-452/R-96-013 (NTIS PB97-115406), Office of Air Quality Planning and Standards, Research Triangle Park, NC, 1996.
4. Wolff, G. T., *Closure by the Clean Air Scientific Advisory Committee (CASAC) on the Staff Paper for Particulate Matter*, EPA-SAB-CASAC-LTR-96-008, U.S. EPA, Washington, DC, 1996.
5. Federal Register, 62 FR 38652, July 18, 1997.
6. Dreher, K., Jaskot, R., Richards, J. H., Lehmann, J. R., Winsett, D., Hoffman, A., and Costa, D., *Am. J. Respir. Crit. Care Med.* 153(4):A15 (1996).
7. Dreher, K., Jaskot, R., Lehmann, J. R., Richards, J. H., McGee, J. K., Ghio, A. J., and Costa, D. L., *J. Toxicol. Environ. Health* 50:285-305 (1997).
8. Miller, C. A., Linak, W. P., King, C., and Wendt, J. O. L., *Combust. Sci. Technol.* 134:477-502 (1998).
9. Garg, S., "EPA Method 0060: Methodology for the Determination of Metals Emissions in Exhaust Gases from Hazardous Waste Incineration and Similar Combustion Processes," in *Methods Manual for Compliance with the BIF Regulations: Burning Hazardous Waste in Boilers and Industrial Furnaces*, EPA/530-SW-91-010 (NTIS PB91-120006), Office of Solid Waste and Emergency Response, Washington, DC, 1990, pp. 3-1 to 3-48.
10. *EPA Test Method 1A: Sample and Velocity Traverses for Stationary Sources with Small Stacks or Ducts*, 40 CFR Part 60 Appendix A, Government Institutes Inc., Rockville, MD, 1994.
11. *EPA Test Method 5: Determination of Particulate Emissions from Stationary Sources*, 40 CFR Part 60 Appendix A, Government Institutes Inc., Rockville, MD, 1994.



12. Galbreath, K. C., Zygarićke, C. J., Huggins, F. E., Huffman, G. P., and Wong, J. L., *Energy Fuels* 12:818–822 (1998).
13. Huggins, F. E., and Huffman, G. P., *J. Hazardous Materials*, 74:1–23 (2000).
14. Linak, W. P., Srivastava, R. K., and Wendt, J. O. L., *Combust. Sci. Technol.* 101(1–6):7–27 (1994).
15. Steele, W. J., Williamson, A. D., and McCain, J. D., *Construction and Operation of a 10 cfm Sampling System with a 10:1 Dilution Ratio for Measuring Condensable Emissions*, EPA/600-8-88-069 (NTIS PB88-198551), Air and Energy Engineering Research Laboratory, Research Triangle Park, NC, 1988.
16. McBride, B. J., Gordon, S., and Reno, M. A., *Coefficients for Calculating Thermodynamic and Transport Properties of Individual Species*, NASA Technical Memorandum 4513, 1993.
17. Chase Jr., M. W., *JANAF Thermochemical Tables, 3rd ed., Parts 1 and 2*, American Institute of Physics, New York, 1986.
18. Barin, I., Knacke, O., and Kubaschewski, O., *Thermochemical Properties of Inorganic Substances*, Springer-Verlag, New York, 1973.
19. Barin, I., Knacke, O., and Kubaschewski, O., *Thermochemical Properties of Inorganic Substances* (supplement), Springer-Verlag, New York, 1977.
20. Barin, I., *Thermochemical Data of Pure Substances*, VCH Verlagsgesellschaft, New York, 1989.
21. Barin, I., *Thermochemical Data of Pure Substances*, VCH Verlagsgesellschaft, New York, 1993.
22. *TAPP: Thermodynamic Properties Software, V2.2*, ES Microwave Inc., Hamilton, OH 1995.
23. Ebbinghaus, B. B., *Combust. Flame* 101:119–137 (1993).
24. Ebbinghaus, B. B., *Combust. Flame*. 93:311–338 (1995).
25. Linak, W. P., and Wendt, J. O. L., *Fuel Process. Technol.* 39:173–198 (1994).
26. Williams, A., *Prog. Energy Combust. Sci.* 2:167–179 (1976).
27. Gelbard, F., and Seinfeld, J. H., *J. Colloid Interface Sci.* 78(2):485–501 (1980).
28. Linak, W. P., and Wendt, J. O. L., *Prog. Energy Combust. Sci.* 19:145–185 (1993).
29. Davis, S. B., Gale, T. K., Wendt, J. O. L., and Linak, W. P., *Proc. Combust. Inst.* 27:1785–1791 (1998).

## COMMENTS

Jerald A. Cole, *GE Energy and Environmental Research, USA*. There seems to be a discrepancy between the particulate emissions data from the fire-tube boiler and the refractory-lined furnace. The total emissions rate from the fire-tube boiler is reputed as only a factor of two greater than from the refractory-lined furnace; yet the LOI of the former is about 90%, while for the latter, LOI was negligible. This, on the surface, seems to suggest a difference in the actual metals emission rate between the two systems despite firing the same fuel.

*Author's Reply.* The 90% LOI levels mentioned were for particles larger than 2.5  $\mu\text{m}$ . LOI levels for the total fire tube boiler samples were somewhat lower, between 60% and 85%. One would expect an LOI level of 50% to explain the fire-tube boiler's PM emission rate being twice that of the refractory-lined combustor, given identical inorganic

content in the fuel. However, the LOI procedure will remove species other than unburned carbon, including S and some of the metals, thereby increasing the % LOI and reducing the remaining mass. LOI does not represent unburned carbon nearly as well for heavy fuel oils (in which the metals are organically bound to the carbon) as for coals, where the metals are much less likely to be organically bound. Note also that 40–60% of the S in the fire-tube boiler PM samples was largely unoxidized organic (thiophenic) S, while in the refractory-lined combustor, almost all of the S was in the form of heavier sulfates, thereby increasing the inorganic mass of the refractory-lined combustor PM compared to that from the fire-tube boiler, even for the same fuel. We feel that the loss of more than carbon in the LOI procedure and the greater oxidation of S in the refractory-lined combustor PM explain the apparent discrepancy.